An effective stress constitutive framework for the prediction of desiccation crack in lime-treated soil: Experimental characterization and constitutive prediction

Nicolas Poncelet [a], Gontran Herrier [b], Bertrand François [a,*]

[a] *Université Libre de Bruxelles, BATir Department, Brussels, Belgium*
[b] *Lhoist Business Innovation center, Nivelles, Belgium*

ABSTRACT

The present work investigates the desiccation effects on a lime-treated silty clay. Original experimental techniques have been developed to control suction conditions (with osmotic technique), to track volume variations and cracks occurrence upon drying. Free and constrained desiccations are performed to evaluate the shrinkage potential (for free drying) and the conditions of desiccation crack triggering (upon constrained drying). Also, indirect tensile tests and uniaxial compression tests are carried out to evaluate the strength and stiffness at various suctions. Those investigations have been performed on natural and lime-treated compacted silty clay in order to emphasize the benefits of the lime treatment in the triggering and/or mitigation of the cracking process. To simulate the field conditions of compaction and obtain specimens having geomechanical properties as close as possible of the real material on site, the particular kneading compaction process in a CBR mould was used, and the final specimens were cut at required sizes with a milling machine numerically controlled by computer (CNC). At the end, generalized effective stress framework with an effective stress parameter χ calibrated according to a power law is used to provide a constitutive interpretation of the occurrence of desiccation cracks in relation with the water retention properties, the soil stiffness, the tensile strength and the geometrical constraints of the soil specimens. It is observed that the cracks initiate under positive (compressive) effective stress. For the used compacted materials, it is demonstrated that the lime treatment postpones the occurrence of desiccation cracks, that are triggered at higher suctions. So, lime treatment plays a favourable role in the reduction of shrinkage and crack occurrence of soft soils subject to drying.

© 2021 Elsevier Ltd. All rights reserved.

1. Introduction

Lime treatment of clayey soil is a well-established technique to improve the engineering properties of soils that have initially poor mechanical properties. Lime treatment influences the soil behaviour on two different time scales. First, lime quickly reacts with clay by modifying its structure, and allowing the clay minerals to flocculate, merge and form larger aggregates. The second effect is a soil stabilization linked to long-term pozzolanic reactions.[1]

As detailed in Refs. 2, 3, desiccation cracking mainly occurs because the shrinkage due to drying is partially or totally constrained by various effects, such as the presence of a less desiccated supporting substrate,[4] a non-uniform drying,[5] the self-equilibrating stress concentrations,[6] the presence of frictional or other traction or displacement boundary conditions[7,8] or intrinsic factors as internal soil texture and structure.[9,10] Upon drying, the suction increases and induces an internal (effective) stress in the materials that tends to produce shrinkage. In order to restrain this shrinkage, a tensile stress is developed in the materials, opposed to the compressive effective stress. Cracks are commonly considered as the consequence of the overpassing of the tensile strength by the generated tensile stress.[2,11–19] If desiccation can produce tensile cracks, it also provides a strength increase and so, an increase of the resistance to crack formation.[20]

Past researches developing dedicated experimental programs were achieved in order to study effects of initial soil density, base adhesion, soil thickness or desiccation rate.[5] Corte and Higashi (1960)[11] performed the first series of most comprehensive laboratory tests on desiccation cracking. While temperature, relative humidity, soil specimen thickness and base material were controlled, the effect of initial density (slurry or loosely compacted soil) was investigated. They observed cracks angles intersection around 120° owing to an energy optimization process.

Lau (1987)[15] performed same kind of test but instrumenting for the first time the soil specimen with embedded ceramic-cup tensiometers in order to measure the suction of the soil during the tests. Dial gauges have also been installed to evaluate the soil surface vertical deformations. Unfortunately, installation of all those measures instruments induced weak points development influencing the cracks triggering. Konrad and Ayad (1997)[4] have also investigated physical processes and pattern evolution of the desiccation cracks on an intact clay. Suction increases induce in a first step primary cracks forming an orthogonal pattern.[5,18,19,21,22] When suction increases moreover, a secondary cracks networks into the blocks of the first pattern. Non orthogonal patterns can also occur when the soil thickness is small and leads to a high concentration of strain energy.[23,24] Sanchez & al. (2013)[25] have also investigated the evolution of the crack network morphology using a 2D profile laser.

Because the lime-treatment of soils affects its shrinkage potential, its stiffness and its tensile strength, the lime treatment modifies, by the way, the propensity of crack occurrence upon drying. On one hand, lime treatment reduces the shrinkage potential but on the other hand, it increases the soil stiffness that, in turn, increases the generated tensile stress induced by deformation constrains. Finally, lime treatment also increases tensile strength. At the end, lime treatment can play antagonist roles and the coupled behaviour including shrinkage potential, soil stiffness and tensile strength must be evaluated separately in order to assess the beneficial or detrimental effects of the lime treatment on desiccation cracking.

Also, during the desiccation process, the material suction continuously changes leading to a change of the material properties. Consequently, those properties (shrinkage potential, stiffness and tensile strength) must be determined, not only as a function of the soil treatment, but also as a function of suction. In this study, suction is controlled by the osmotic techniques from 0 to 1500 kPa.

This paper first presents the constitutive framework using the concept of generalized effective stress for unsaturated soils. In such a way the governing parameters are highlighted. In order to determine those parameters, some specific experimental apparatus have been developed and are presented in the next sections. Also, in the same section, the procedure for soil specimen preparation (through kneading compactions and cutting with CNC machines) is introduced. Finally, experimental results, from indirect tensile tests, uniaxial compression tests and free and constrained desiccations, are presented and interpreted in the light of the developed constitutive framework and conclusions are drawn in regards with the beneficial effect of lime treatment on the reduction of crack initiation.

2. Constitutive framework

In this study, generalized effective stress for unsaturated soil is used with the effective stress parameter χ expressed according to a power law of the degree of saturation[26]:

$$\sigma'_{ij} = \sigma_{net,ij} + \chi.s.\delta_{ij} \tag{1}$$

where σ' is the generalized effective stress, σ_{net} is the net stress, s is the applied suction and χ is a power law of the degree of saturation S_r given in Eq. (2).[27]

$$\chi = S_r{}^\alpha \tag{2}$$

The saturation degree S_r can be related to suction s through the water retention curve for which a Van Genuchthen expression is used[28]:

$$S_r = \left[1 + \left(\frac{s}{P_r}\right)^n\right]^{(1 - \frac{1}{n})} \tag{3}$$

where n and P_r are two material parameters.

The stress–strain behaviour is considered elastic:

$$d\varepsilon_{ij} = C_{ijkl}.d\sigma'_{kl} \tag{4}$$

where ε is the strain and C the compliance matrix, governed, classically, by Young modulus and Poisson ratio. The Young modulus is a function of suction, through non-linear elasticity.

Upon free shrinkage, the deformation is free of external (net) stress and the strain is fully induced by the variation of effective stress, linked to the change of suction and degree of saturation. According to the elastic law, the strain increment vector can be expressed as:

$$\begin{pmatrix} d\varepsilon_1 \\ d\varepsilon_2 \\ d\varepsilon_3 \end{pmatrix} = \frac{1}{E(s)} \begin{pmatrix} 1 & -\upsilon & -\upsilon \\ -\upsilon & 1 & -\upsilon \\ -\upsilon & -\upsilon & 1 \end{pmatrix} \begin{pmatrix} d\left[(S_r)^\alpha.s\right] \\ d\left[(S_r)^\alpha.s\right] \\ d\left[(S_r)^\alpha.s\right] \end{pmatrix} \tag{5}$$

For constrained shrinkage, the deformation is fully blocked in both horizontal directions (directions 1 and 2) while the vertical direction (direction 3) is free to shrink. Those restrictions induce an increase of external (net) stress according to the elastic law:

$$\begin{pmatrix} 0 \\ 0 \\ d\varepsilon_3 \end{pmatrix} = \frac{1}{E(s)} \begin{pmatrix} 1 & -\upsilon & -\upsilon \\ -\upsilon & 1 & -\upsilon \\ -\upsilon & -\upsilon & 1 \end{pmatrix} \begin{pmatrix} d\left[\sigma_{net,1} + (S_r)^\alpha.s\right] \\ d\left[\sigma_{net,2} + (S_r)^\alpha.s\right] \\ d\left[(S_r)^\alpha.s\right] \end{pmatrix} \tag{6}$$

In Eq. (6), the unknowns are $d\sigma_{net,1}$, $d\sigma_{net,2}$ and $d\varepsilon_3$. For a suction-controlled problem, the materials parameters that must be determined are the elastic parameters (Young modulus evolving with suction and Poisson ratio), the α coefficient and the retention curve parameters (to deduce the degree of saturation for any suction). Young modulus can be measured on uniaxial compression tests performed at various suction while the α coefficient is fitted to fulfil the uniqueness of the shear failure criterion expressed in this effective stress formalism, whatever the suction level. This is done from uniaxial compression strength at various suctions according to the methodology developed by Gerard et al. (2015)[27] (see Section 5.1 for more details). The retention curve parameters are obtained by fitting the Van Genuchten expression (Eq. (3)) on experimental results obtained from a dewpoint potentiometer.

3. Materials and experimental methods

3.1. Soil properties

A silty clay soil (CL, according to the Unified Soil Classification System − USCS) that has been used for the construction of a prototype dike in the South of France has been chosen for this study. Its index properties are: liquid limit (w_L) = 33,6%; plasticity index (IP) = 14.8%. The clayey fraction represents 22%, the silty one about 60% and the sandy one about 18%. This material has shown its relevance to be treated with lime, essentially due to its relatively large clay fraction.

The lime-treated soils are tested with a treatment with 2% of lime, after 7 days of curing, that correspond to the conditions of the prototype dike, on site. A quicklime CL 90-Q (according to standard EN 459-1) from the Lhoist group was used (Particle sizes: 99,98% < 2 mm and 83% < 80 μm; Available lime content: 91,2%; Reactivity: t_{60} = 4–6 min).

Optimum normal proctor conditions have been determined at w_{opt} = 15.5 % and $\gamma_{d,opt}$ = 17.6 kN/m^3 for untreated soil and w_{opt} = 17.8 % and $\gamma_{d,opt}$ = 17.1 kN/m^3 for soil treated soil with 2% of lime.

The water retention curves of both treated and untreated materials are reported in Fig. 1. They have been determined on small fragments of compacted soils (see compaction process in Section 3.2). Osmotic technique was used to insure a fine control of the suction for suctions lower than 1 MPa. For greater suctions,

N. Poncelet, G. Herrier and B. François

Table 1
Van Genuchten parameters for both untreated and treated soils after 7 days of curing.

	P_r [-]	N [-]
Untreated soils	120 000	1.18
Lime treated soils	75 000	1.25

Table 2
Skempton coefficient after the last saturation step.

Confining pressure, σ_3 [kPa]	Skempton coefficient, $\overline{B}$ [%]	
	Untreated	Treated
50	96,5	99,86
100	94,75	97,5
200	96,67	97,5

Table 3
Effective friction angle ϕ' and cohesion c' of treated and untreated specimens at 7 days of curing.

	ϕ' [°]	c' [kPa]
Untreated soils	32.7	1.8
Lime treated soils	34.9	71.5

specimens are dried under free air conditions during various lapses of time (from a couple of minutes to several hours) and then placed 24 h in hermetically sealed containers to obtain a global homogenization of water distribution in the specimen. They are then inserted in a dewpoint potentiometer to measure their total suction.

The experimental points are fitted through the Van Genuchten model (Eq. (3)) with the best-fit parameters n and P_r, in the least-square sense, given in Table 1.

In addition, consolidated undrained triaxial tests, with measurement of pore water pressure, have been performed in order to obtain the effective friction angle ϕ' and effective cohesion c' for treated and untreated specimens. Three confining pressures have been investigated in both cases (50 kPa, 100 kPa and 200 kPa). After shaping the specimen (as detailed in Section 3.2), the samples are saturated by increasing the confining pressure and the backpressure (water pressure). During this saturation process, a confining pressure of 30 kPa in excess to the backpressure, is kept in order to insure its internal stability. The saturation is achieved step by step by increasing of 50 kPa the confining pressure and the back pressure simultaneously. After each step, the Skempton Coefficient $\overline{B}$ is recorded in order to evaluate the saturation condition of the sample. The values of this coefficient are given for untreated and lime-treated samples after the last saturation step in Table 2.

Obtained Skempton coefficients being higher or very close to 0.97 (excepted for the untreated specimen submitted subsequently to 100 kPa of confining pressure, for which it was not possible to go higher than 0.9475), the samples can be assumed well-saturated. When this saturation process is completed, the consolidation (drained process) begins in order to obtain the final desired confining pressure.

After the consolidation, and respecting a curing time of 7 days for the treated samples, the undrained uniaxial compression test is performed with a constant vertical displacement rate of 0.01667 mm/min. In addition to the vertical displacement recorded with an LVDT, the load apply on the sample and the internal water pressure are also recorded.

The results of these tests are presented in Figs. 2 to 7 through the evolution of the deviatoric stress q in function of the axial strain ε_1, the evolution of the water pressure u_w in function of the axial strain ε_1 and the deviatoric stress q in function of the mean effective stress p' for untreated (Figs. 2 to 4) and lime treated (Figs. 5 to 7) specimens after 7 days of curing time.

The failure criterion selected, marked by a red square in Figs. 4 and 7 for each confining pressure, corresponds to the conditions when the ratio of σ_1' by σ_3' is maximum.[29,30]

From these results, effective friction angle ϕ' and cohesion c' have been deduced as summarized in Table 3.

3.2. Specimens preparation

For the soil preparation, the dry soil is mixed with the required quantity of water to reach an initial water content of 16% for untreated soil and 21.5% for treated soil. After wetting the soil at targeted water content, wet soil is sealed in plastic buckets during at least 24 h to achieve homogeneous water content in the soil. Then, after addition of 2% of lime, the treated soil loose approximately 1.7% of water content to reach the targeted initial water content of 19.8%. Treated soil is then sealed in a bucked during one hour before compaction.

In order to simulate the action of compacting machinery in the field, the kneading compaction[31] has been used for specimen preparation. It is based on the use of a three kneading feet tool designed to fit with a CBR mould (15.24 cm diameter and 12.7 cm height) and mounted on a mechanical press. The total soil volume needed to realize a CBR specimen is divided in five layers. Each of them is then compacted with an eight steps compaction sequence. The target values of the dry unit weight γ_d are respectively 1,71 g/cm^3 and 1,64 g/cm^3 for untreated and treated soil. To achieve this target density, the stress applied on the layers during each compaction step is equal to 0.45 and 0.65 MPa respectively for the untreated and the treated soil.

Finally, from CBR specimens, three kinds of specimens have been extracted:

i. Rectangular specimens (for free and constrained desiccations) of 140 mm length, 50 mm width and 15 mm height
ii. Cylindrical specimens (for indirect tensile tests) of 36 mm diameter and 18 mm height.
iii. Cylindrical specimens (for uniaxial compression tests) of 36 mm diameter and 72 mm height.

In order to avoid soil damaging during specimen extraction from the CBR model and also to obtain precise specimen dimensions, specimen have been cut with a milling machine numerically controlled by a computer including a CAD step as shown on Fig. 8. The specimen is first drawn on conventional 3D CAD software and GCodes are created with specific tools in order to drive the milling machine. Precision and versatility in the possible shapes of specimens is a strong asset of the method. At the end, the specimen size and volume are measured using a 3D scanner ensuring no strain or damage due to contact with conventional measurement tools.

3.3. Desiccation system

For our application, suction control by osmotic technique[11] has been selected as the most appropriate method to control the suction of the specimens mainly for two reasons. On one hand, this technique offers a good precision in the suction control for the range of applied suction concerned in this study (0 to 2 MPa), i.e. suction range at which the cracks occur. On the other hand, the time to reach suction equilibrium in the specimens remains lower than the 7 curing days selected as a target for all the tests on treated materials.

The purpose here is to control the suction of the soil specimen while the specimen is drying upon free or constrained conditions.
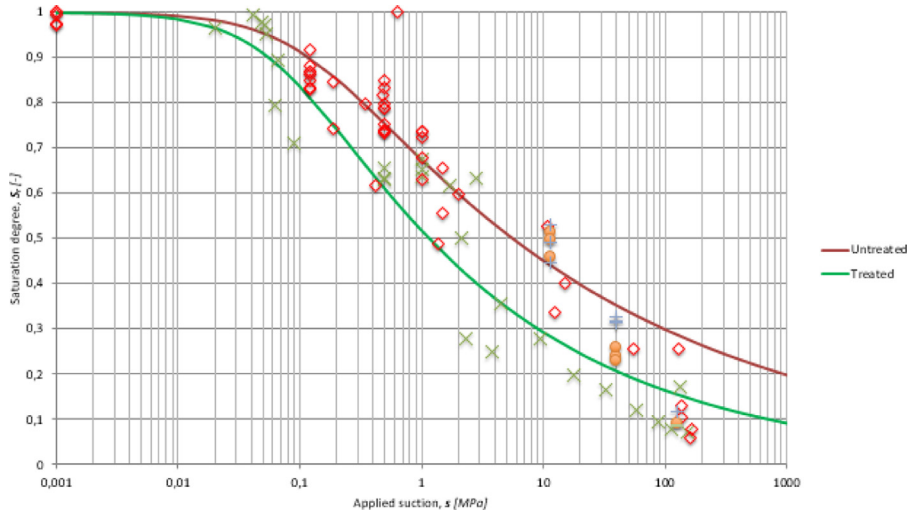
N. Poncelet, G. Herrier and B. François

Fig. 1. Water retention curve (WRC) of both treated and untreated soils.
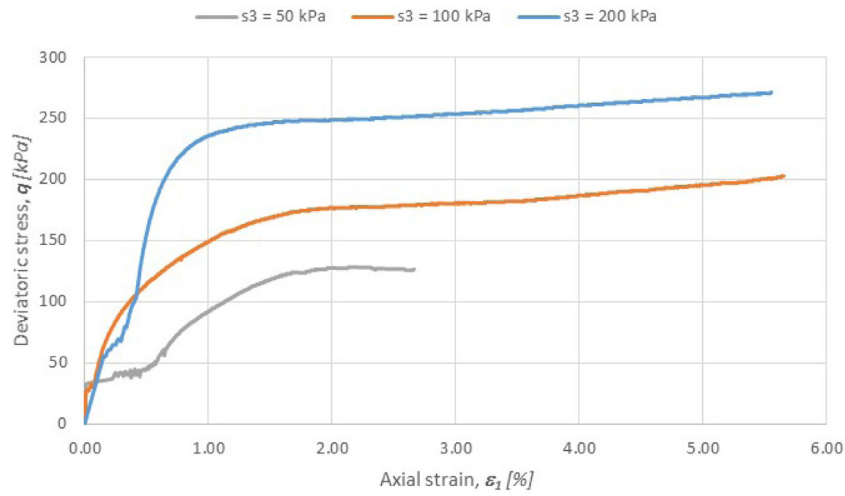

Fig. 2. Deviatoric stress q in function of the axial strain ε_1 for each confining pressure of untreated samples.
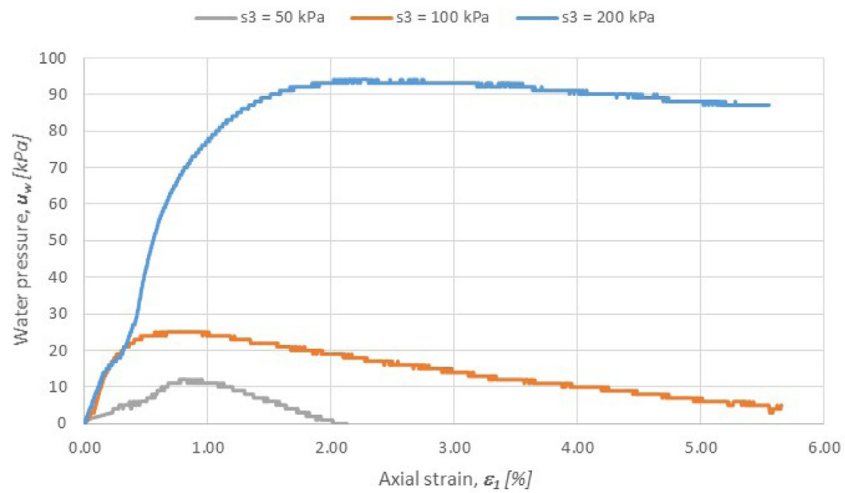

Fig. 3. Water pressure u_w in function of the axial strain ε_1 for each confining pressure of untreated samples.
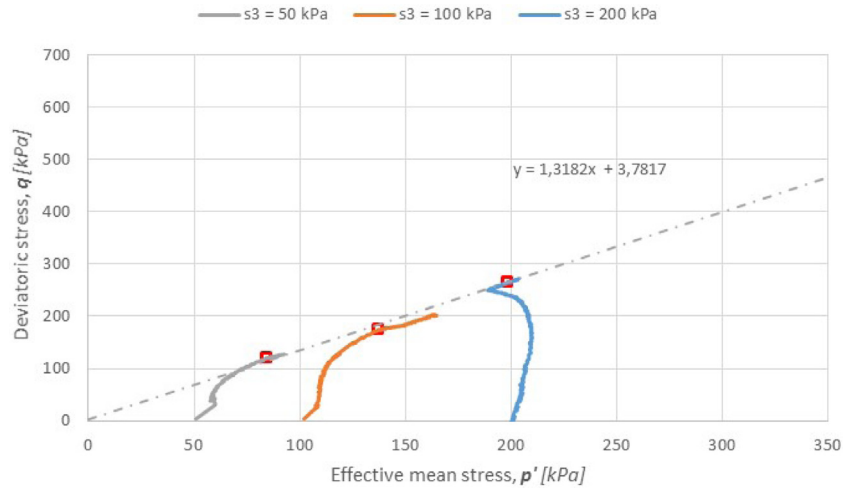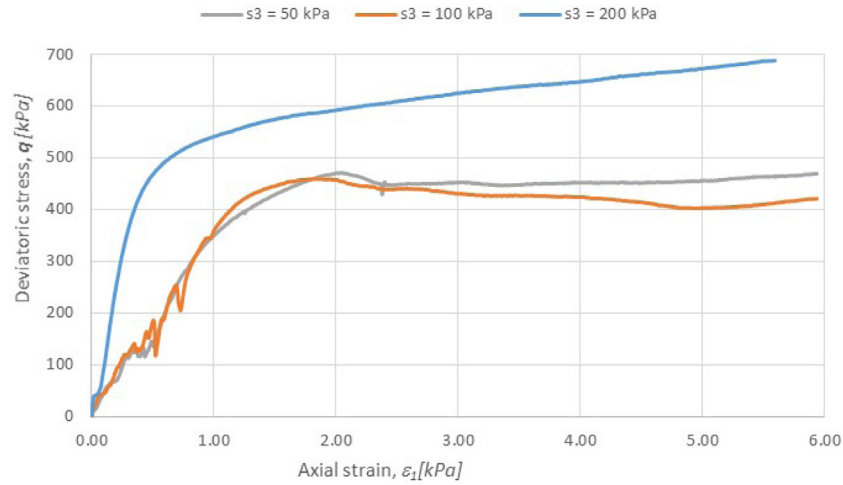
N. Poncelet, G. Herrier and B. François

Fig. 4. Consolidated undrained triaxial tests results of untreated specimens. Stress path in the (p′ -q) plane.

Fig. 5. Deviatoric stress q in function of the axial strain ε_1 for each confining pressure of treated samples.
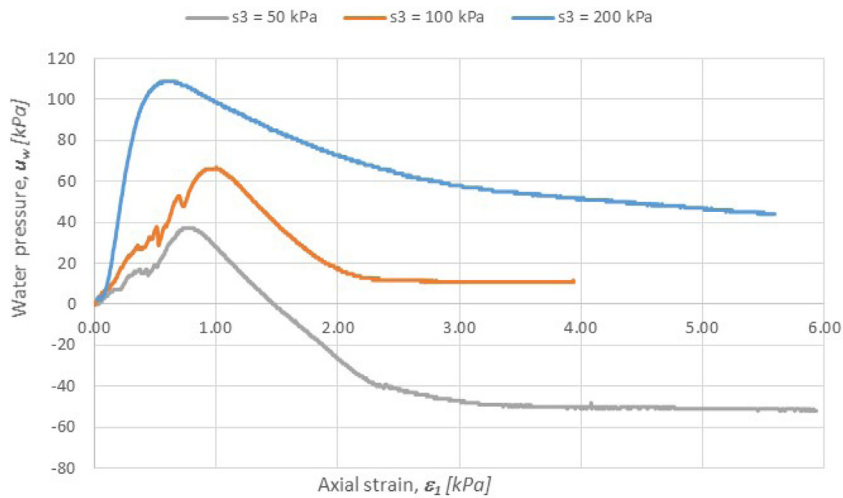
Fig. 6. Water pressure u_w in function of the axial strain ε_1 for each confining pressure of untreated samples.

Consequently, the osmotic system for the suction application must be combined with a constraining frame that blocks any soil deformation in the horizontal direction. Consequently, a specific osmotic device was developed to reproduce the drying process from one face of the specimen and possible deformation restriction on the other face. A solution of Poly-Ethylene Glycol (PEG)
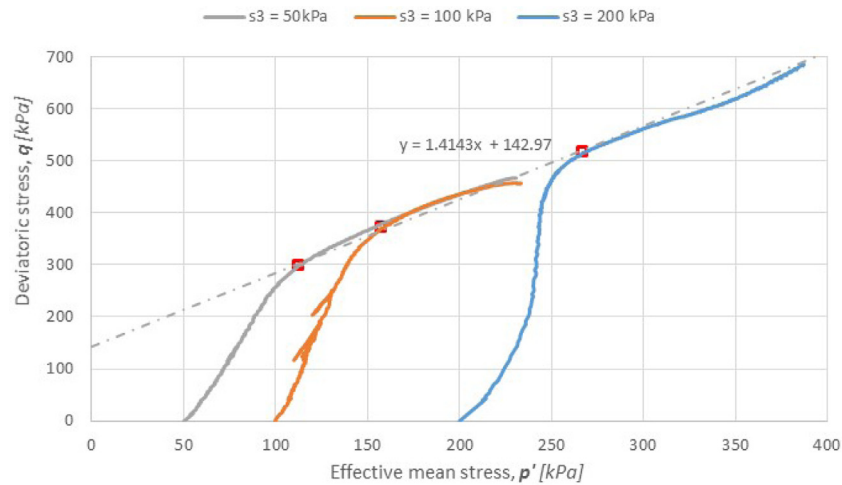
Fig. 7. Consolidated undrained triaxial tests results of treated specimens after 7 days of curing. Stress path in the (p′−q) plane.
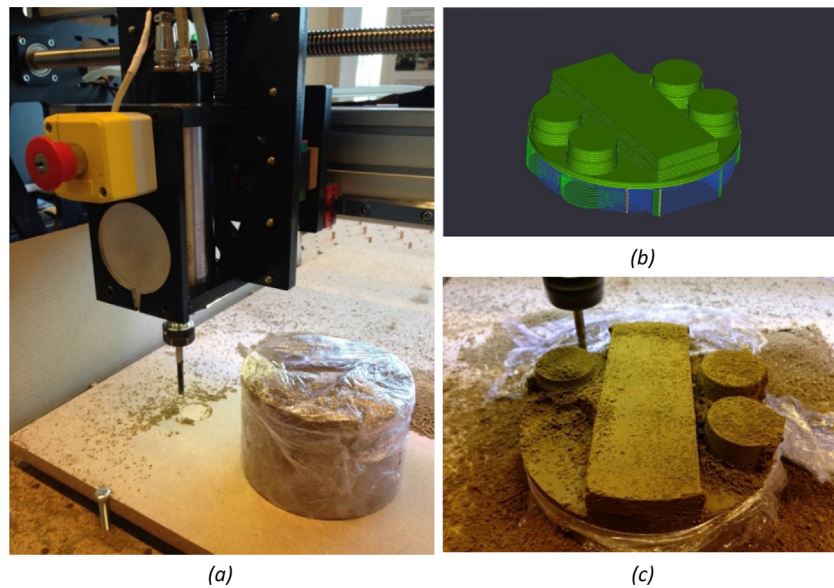

Fig. 8. Milling machine numerically controlled (a) using a CAD step (b) to obtain particular specimens with high definition (c).

in various concentrations circulates in a circuit under a flat semi-permeable membrane while the specimens are installed on that membrane (Fig. 9).

In case of constrained shrinkage, a two-dimensional truss with 122 pines made in a single piece of aluminium is introduced on the top surface of the specimen. Each pine has a diameter of 1.0 mm and a height of 2.0 mm (Fig. 10).

This system allows to constrain the horizontal strain at the base of the specimen while the vertical strain is remained free. The high density of pines allows to minimize the stress concentration on the soil around each pine during the constrained desiccation process. At the end, it was observed that the cracks initiate from the opposed side to the pines (the side submitted to drying) while the pine does not produce crack triggering due to a possible stress concentration.

3.4. Experimental program

The objective of the experimental program is to evaluate the shrinkage or swelling behaviour from as-compacted conditions to various targeted suction levels. Free and constrained swellings/shrinkages of untreated and lime treated soil specimen

are monitored under various target suctions (each 500 kPa from 0 to 1500 kPa and the as compacted suction). Under free conditions, the specimen dimensions are measured with the 3D scanner while for constrained conditions, the occurrence of cracks is monitored visually. Also, compressive and tensile strength are evaluated respectively through uniaxial compressive tests and indirect tensile tests.[32] In addition of the previous suction levels, the as-compacted state corresponding to a suction of 120 kPa is also investigated during these testing procedures. For treated soils, the behaviour is characterized after 7 days of curing time as discussed previously. The curing takes place in parallel with the suction equilibration in the specimen.

In parallel to those free and constrained desiccation, conventional uniaxial compression tests and indirect tensile tests (i.e. Brazilian tests) have been performed on specimen at various suctions. Here again, suction was imposed by the osmotic technique, by immersing the specimen, surrounded by sealed semi-permeable membrane in a solution of Poly-Ethylene Glycol (PEG) in various concentrations, depending on the desired applied suction. Table 4 summarizes the performed tests and their respective conditions in terms of treatment and suction.
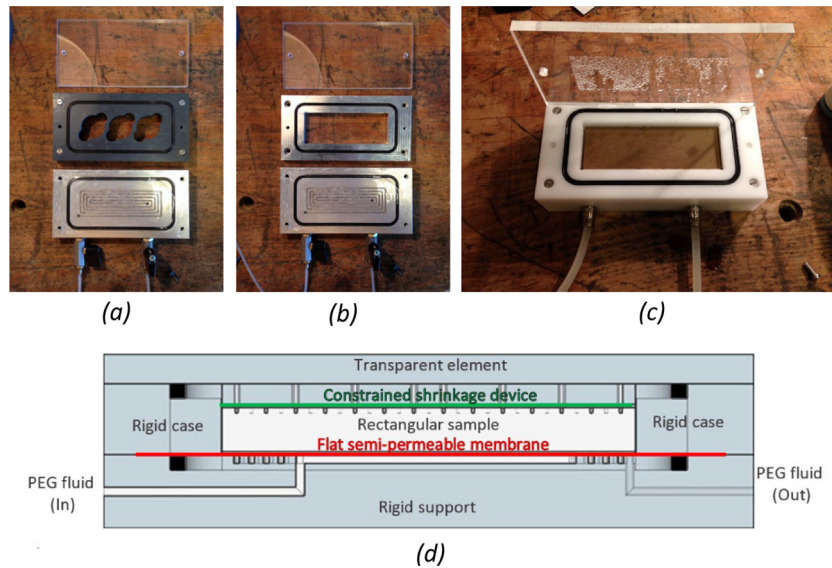
Fig. 9. Detail of the desiccation device for the indirect tensile test specimens (a) and free or constrained shrinkage test specimens (b). Global overview (c) and cutting section (d) of the assembled system.
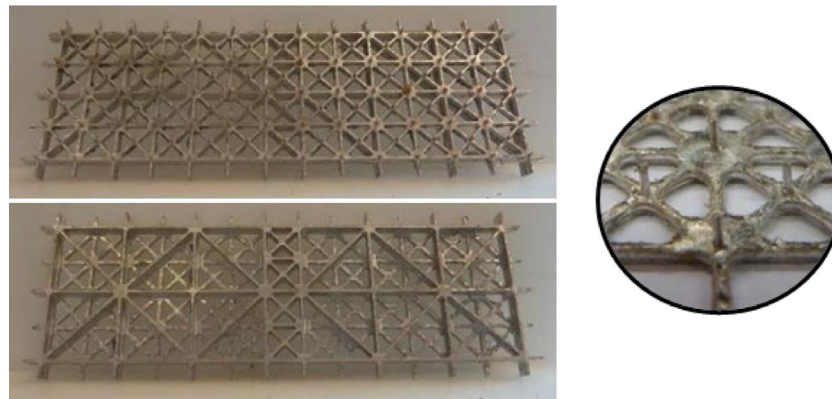

Fig. 10. Top and bottom view of the constrained shrinkage devise (CSD) (left) and zoom on the pines (right).

Table 4
Summary of the experimental program.

		Suction [kPa]				
		0	120	500	1000	1500
Treatment	Treated	3 B.T.	3 B.T.1	3 B.T.	3 B.T.	4 B.T.
		1 C.S.	C.S.1	1 C.S.	1 C.S.	1 C.S.
		1 F.S.	F.S.2	1 F.S.	1 F.S.	1 F.S.
		1 U.C.	U.C.	2 U.C.	2 U.C.	2 U.C.
	Untreated	3 B.T.	3 B.T.	3 B.T.	3 B.T.	
		1 C.S.	1 C.S.	1 C.S.	1 C.S.	4 B.T.
		1 F.S.	1 F.S.	1 F.S.	1 F.S.	2 U.C.
			2 U.C.	2 U.C.	2 U.C.	

B.T.: Brazilian tests; C.S.: constrained shrinkage; F.S.: free shrinkage; U.C.: uniaxial compression.

4. Results

4.1. Indirect tensile tests

The tensile strength, determined from indirect tensile tests, is strongly affected by lime treatment and suction. Fig. 11 shows the evolution of the tensile strength as a function of the applied suction, for treated (after 7 days of curing time) and untreated specimen. As expected, tensile strength increases with suction in the case of untreated specimens. However, oppositely, tensile strength of the treated specimens is not significantly affected by suction and oscillates around 90 kPa, excepted for saturated specimen exhibiting a much lower tensile strength. We also observe a spreading of the results due to the variability of dry density (the kneading compaction process induces a slight heterogeneity in the obtained density). Fig. 12 shows the same tensile strength results in function of the applied suction and underlines an important aspect of the lime treatment. For treated specimens, the increase of the tensile strength seems to be more linked to an increase of the dry bulk density rather than an increase of suction. Specimens subjected to low suction may indeed develop greater tensile strength than ones subjected to strong suction if their dry bulk density are greater.

4.2. Uniaxial compression tests

Fig. 13 presents the compressive strength of the treated and untreated specimens subjected to the same range of suction, from 0 to 1500 kPa. The increase of the suction induces an increase of the compressive strength for both treated and untreated specimens. The uniaxial compression test of untreated specimen under saturated conditions was not performed because of the too soft character of the specimen.
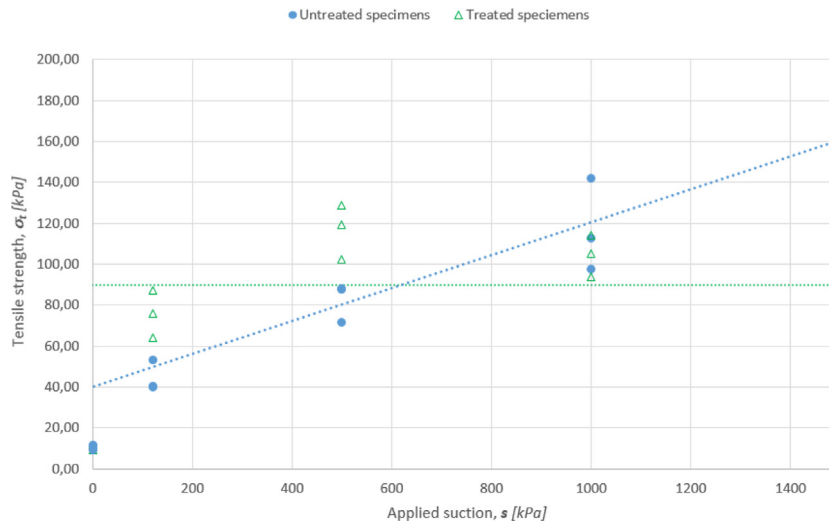
Fig. 11. Tensile strength σ_t in function of the applied suction s.
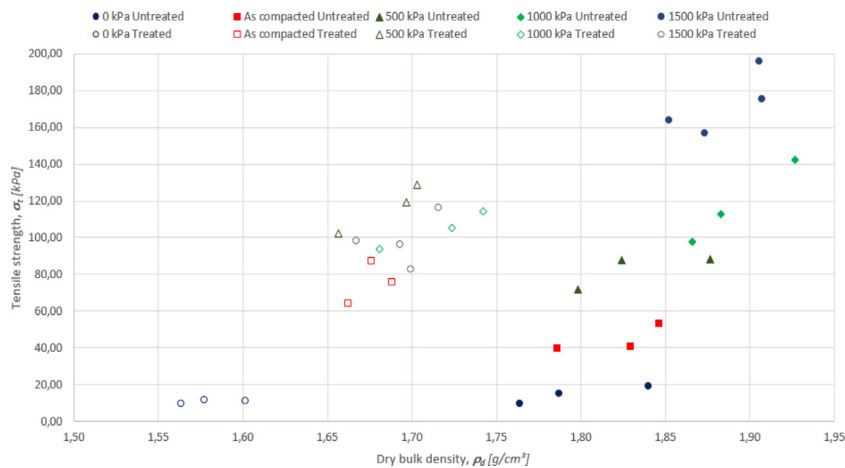

Fig. 12. Tensile strength σ_t in function of the dry bulk density γ_d.

Fig. 14 presents the Young modulus obtained at the inflection point of the uniaxial compression curve respectively for untreated and treated specimens. The start of the curve being affected by the progressive contact between the piston and the soil specimen, the slope around the inflection point has been selected as the most representative value of the stiffness of the material. Slopes have been calculated on each strain interval of 0.1%, the maximum value gives the desired Young modulus E. It is obtained in the same range of strain than the one experienced by the material during drying. We may observe that the suction level has a significant impact on the Young modulus of both treated and untreated specimens. The suction increase induces an increase of the Young modulus.

4.3. Free shrinkage

With the 3D scanner, the volume of the specimens was measured before and after suction application for free shrinkage of parallelepiped specimens and small cylindrical specimens. Obtained results are shown on Fig. 15 where UCS and TCS mean respectively Untreated and Treated Cylindrical specimens while UPS, and TPS mean respectively Untreated and Treated Parallelepipedal specimens. It underlined first that lime-treatment reduces significantly the volume variations (swelling or shrinkage) of the specimen. Secondly, for each suction level and treatment,

volumetric strains ε_v are in the same range of value. The shape of the specimen does not affect the volume variation upon drying. For the "as-compacted" conditions corresponding to 120 kPa of suction (without any change during 7 days), untreated soils show no volume variation while treated soils exhibit a slight endogenous shrinkage, due to lime reaction.

4.4. Constrained shrinkage

For constrained shrinkage, the deformation is restricted with the two-dimensional truss with pines introduced in the top surface of the specimens. Possible cracks occurrence is observed visually. As summarized in Table 5, desiccation cracking occurs for the drying at a suction of respectively 1000 kPa and 1500 kPa on untreated and treated soils. A single crack develops perpendicularly to the larger direction of the specimen, approximately in the middle (Fig. 16).

5. Constitutive interpretation

5.1. Calibration of the α parameter

According to the approach developed by Gerard et al. (2015),[27] it is possible to deduce the exponent α of the effective stress
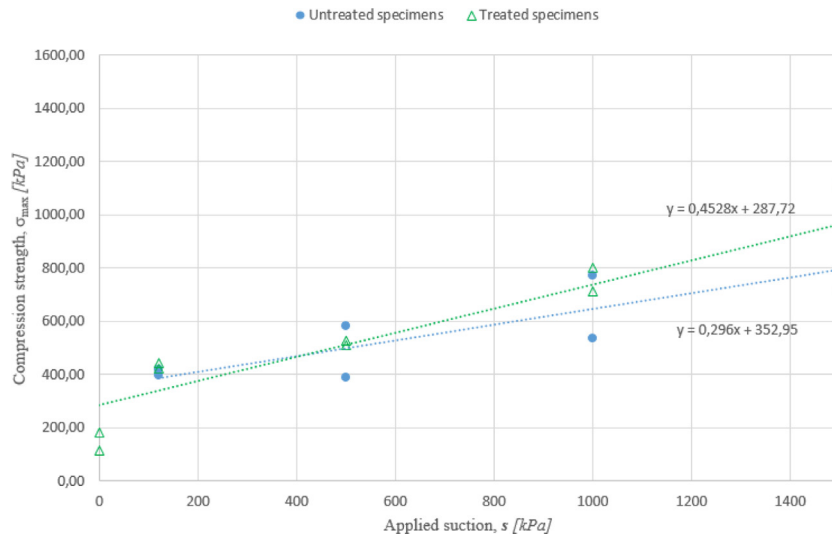
Fig. 13. Compressive strength in function of the applied suction. Experimental measurements (points) and fitted linear evolutions (dotted lines).
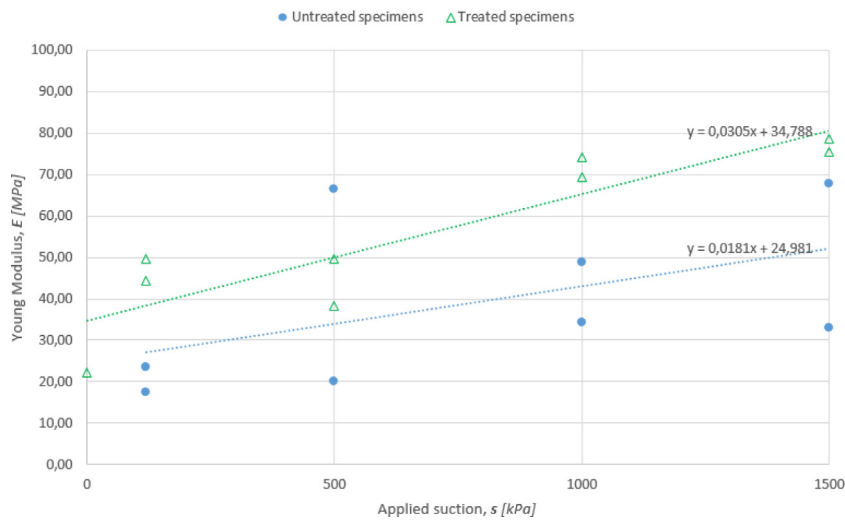

Fig. 14. Young modulus in function of the applied suction. Experimental measurements (points) and fitted linear evolutions (lines).
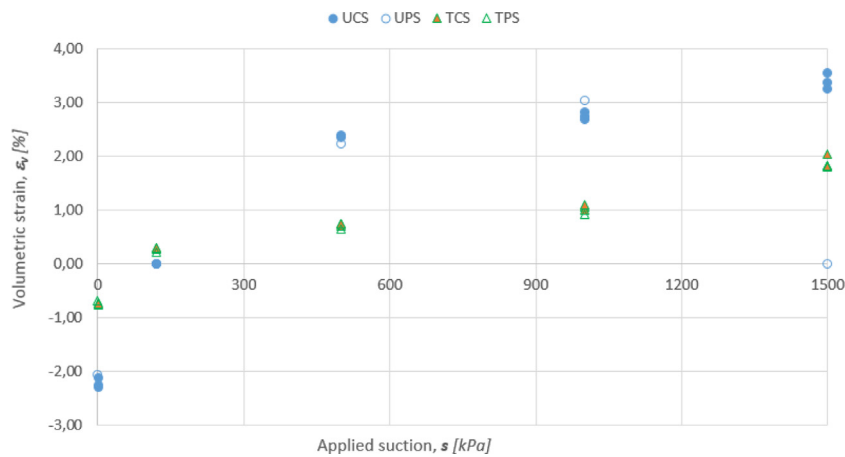

Fig. 15. Volumetric strain ε_v in function of the applied suction s for both treated and untreated samples. UCS: Untreated Cylindrical Specimens; TCS: Treated Cylindrical Specimens; UPS: Untreated Parallelepiped Specimens; TPS: Treated Parallelepiped Specimens.

parameter in order to obtain the uniqueness of the failure criterion for any suction. The purpose being to obtain an unique

failure criterion, the objective is to find the value of χ, expressed as a function of S_r as detailed in Eq. (2), that allows to shift

Fig. 16. Crack observed on the treated sample subject to a suction of 1500 kPa. Right: crack triggering from the dried surface.
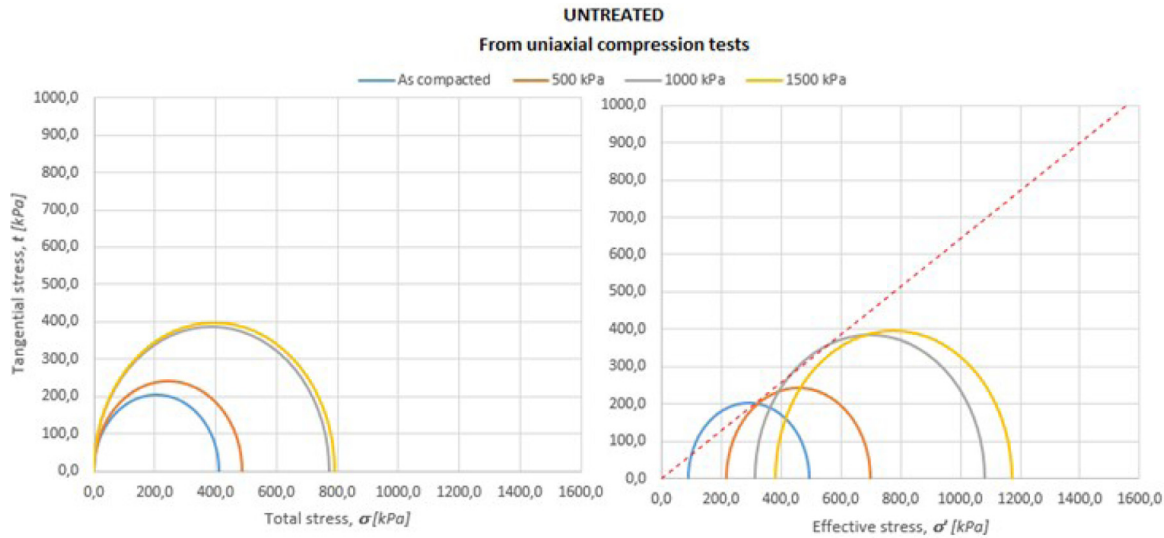

Fig. 17. Calibration of the function χ for untreated soil ($\alpha = 2.97$) from uniaxial compression tests. Left: Mohr circle at failure in the total stress reference; Right: Mohr circle at failure and failure criterion in the effective stress reference.

Table 5
Visual observation of the cracks during the various tests.

Applied suction	Treatment	
	Untreated	Treated
0 kPa	✕	✕
As compacted	✕	✕
500 kPa	✕	✕
1000 kPa	✓	✕
1500 kPa	–	✓

horizontally the corresponding Mohr circle at the ultimate stress state expressed in total stress on the failure criterion, expressed in effective stress.

The intrinsic strength is given by the effective strength upon saturated conditions ($\phi' = 32.7°$ and $c' = 1.8$ kPa for untreated soils; $\phi' = 35.7°$ and $c' = 71.9$ kPa for treated soils) and the distance between saturated strength and strengths at different suctions is compensated by the product $\chi \cdot s$.

The best fit, in the sense of least square, to get the uniqueness of the failure criterion is obtained for $\alpha = 2.97$ for untreated soils and $\alpha = 2.68$ for treated soils. Figs. 17 and 18 show the obtained alignment of the uniaxial compression stress failure circles in the effective stress reference.

Fig. 19 shows the obtained relationship between χ and S_r for treated and untreated soils and compares it with the values $\alpha = 2.08$ obtained by Gerard & al. (2015) on a similar (untreated) compacted silty soil.

According to Alonso et al.[26], the obtained curve between χ and S_r is related to the double structure of the soils, induced by the mode of soil preparation (compaction in this case). Due to this double structure, with two characteristic sizes of pores (large pores between aggregates and small pores inside aggregates) upon low degree of saturation, the water is essentially stored inside the aggregates and this "intra-aggregate' water does not contribute to the macroscopic stress. Upon higher degree of saturation, water floods the "inter-aggregate" voids which contributes more to the increase of the internal stress. By comparison with soil compaction in mould that induces a significant aggregation of particles for treated soils, the kneading effect of the compaction process used in this work lead to a better homogeneity of the soil texture without this "double-structure" aspect, as highlighted in Fig. 20.

In addition, treated samples have been compacted at water content exceeding 2% of the optimum moisture content (on the wet side) in order to obtain better grain lubrication and reduce macropores. The same process was used for the untreated samples but using an exceeding water content of 0.5%. This compaction on the wet side of optimum of treated soils led to a reduced double-structure character of the treated soil corresponding to a smaller value of α.

5.2. Free shrinkage

When the expression of effective stress is known, we can use the elastic stiffness as a function of suction, as determined in Fig. 14, in order to reproduce the strain upon free shrinkage according to Eq. (3). Results are illustrated in Figs. 21 and 22, for untreated and treated specimen, respectively. We assume a Poisson coefficient of 0.2 for both untreated soils and treated soils. Note that for treated soil, an endogenous volumetric shrinkage
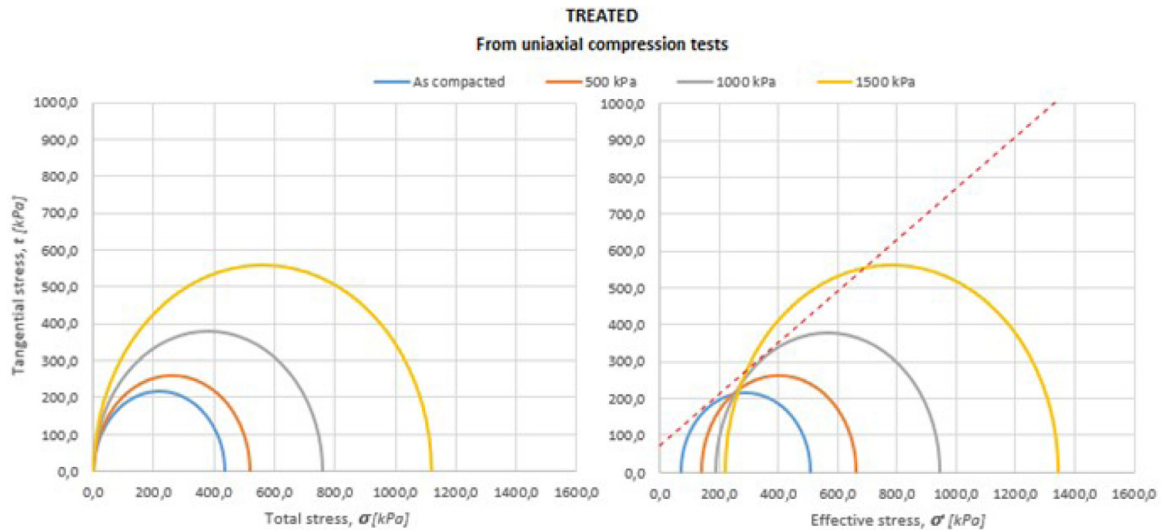
Fig. 18. Calibration of the function χ for treated soil ($\alpha = 2.68$) from uniaxial compression tests. Left: Mohr circle at failure in the total stress reference; Right: Mohr circle at failure and failure criterion in the effective stress reference.
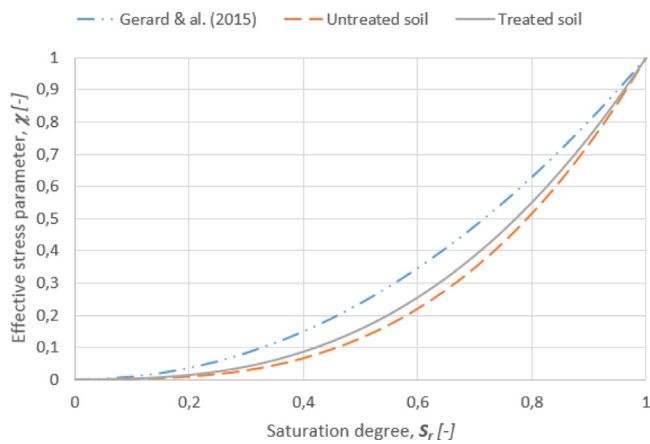

Fig. 19. Comparison of the effective stress parameters χ with the previous study of Gerard et al. (2015).

Fig. 20. Difference between soil structure of treated samples obtained by kneading compaction (left) and compaction in mould (right).

(due to lime reaction with soil) of 0.5% (as observed experimentally for the as-compacted conditions) has been added in all predicted strains.

The model results are obtained exclusively from blind predictions. The elastic stiffness, measured on uniaxial compression tests, is able to reproduce the free shrinkage experienced upon drying process even if slightly underestimated. This small underestimation can be linked to the use of a Young Modulus obtained at 7 days of treatment and considering as a constant during all

the curing time. However, the strains are mainly produced in the early stages of drying at a curing time shorter than 7 days. In a sense, this matching confirms the validity of the α exponent determined independently.

5.3. Constrained shrinkage

Upon constrained shrinkage, Eq. (6) allows to deduce the tensile net stress as a function of suction while the tensile strength is reported in Fig. 11. The comparison of the generated net stress and the strength allows to predict the suction leading to the triggering of desiccation cracking. This is done in Figs. 23 and 24 for untreated and treated soils, respectively.

The zero net stress state corresponds to the as-compacted suction (i.e. 120 kPa). Then, upon constrained conditions when suction decreases (due to wetting), the constrained swelling induces a compressive net stress while when suction increases (due to drying), tensile net stress is induced.

Those developments reveal that, according to this theory, the tensile cracking induced by a desiccation process of the studied soil from as-compacted conditions, under constrained shrinkage, should occur at suctions around 700 kPa for untreated soil and 1200 kPa for treated soil. This is consistent with the experimental observations where we observed that cracks occurred between 500 kPa and 1000 kPa for untreated specimen and between 1000 kPa and 1500 kPa for treated specimen (see Table 4).

Those comparisons between generated tensile stress and tensile strength are valid in both net and effective stress references as shown in Figs. 23 and 24. The net stress representation has the advantage to correspond to the directly-measured tensile strength (net stress being the controlled stress in laboratory) while effective stress is more convenient for the prediction of the generated stress (because the constitutive framework uses the effective stress). However, the passage from net to effective stresses can be done easily when suction, degree of saturation and α exponent are known, according to Eq. (1).

We may also note that the tensile failure occurs upon positive (compressive) range of effective stress. Even if counter-intuitive, this feature was already observed by other studies focusing on desiccation cracking through effective stress analysis.[33,34] Interestingly, Hueckel et al.[35] proposes a plausible explanation for this fact. They demonstrate that, even if the effective stress evaluated at macro-scale is in the compressive range, air entry mechanism
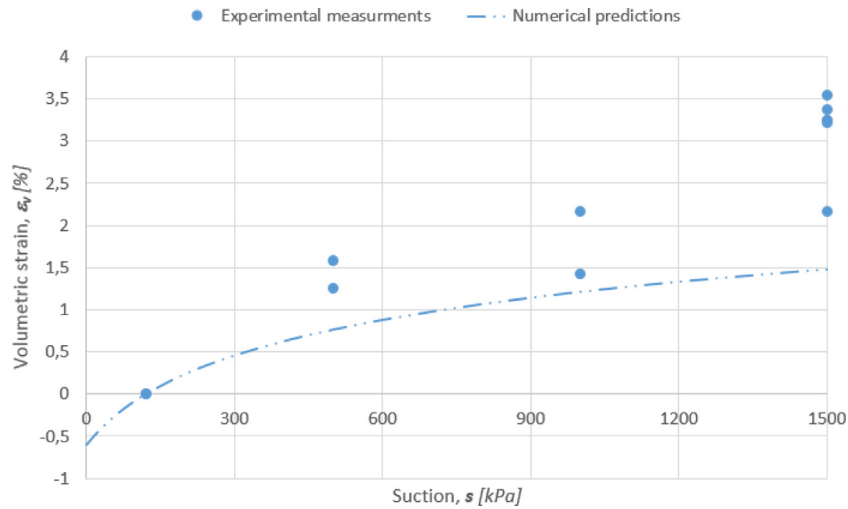
Fig. 21. Comparison between predicted and measured volumetric strains induced by different suctions under free shrinkage on untreated specimen.
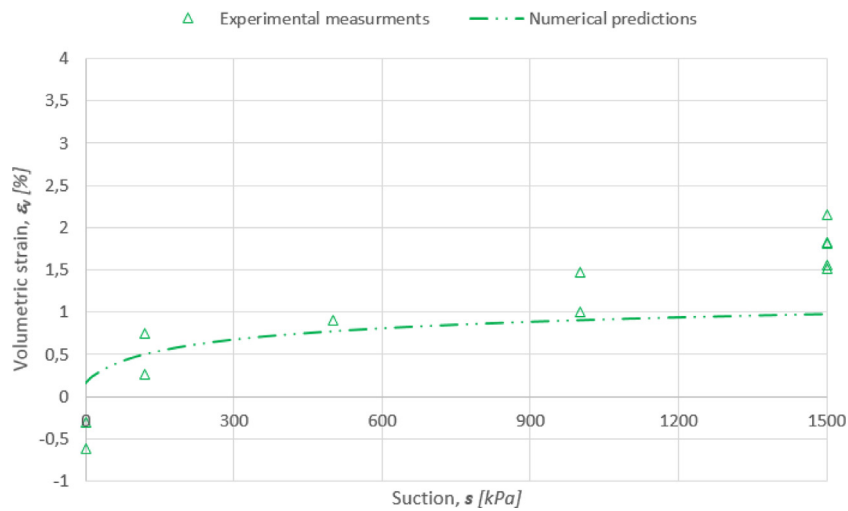

Fig. 22. Comparison between predicted and measured volumetric strains induced by different suctions under free shrinkage on lime treated specimen.

in the pores may generate, at meso-scale, a stress concentration that produces local tensile effective stress and induces the crack initiation.

In this methodology, it is to note that the tensile failure condition is deduced from the indirect tensile test with an encountered stress state at failure that slightly differs from the stress state upon cracking during desiccation. However, indirect tensile test was chosen to characterize the tensile strength of the soil specimen for several reasons. First, it is a test that is particularly well-adapted for lime-treated soils, experiencing relatively brittle failure. Secondly, some comparative studies performed by various authors between tensile strength obtained from indirect tensile tests and direct tensile tests revealed that the obtained tensile strengths may differ due to several parameters, not only related to the different stress states. In particular, Araki et al. (2016)[36] shows that the difference on tensile strength of compacted soils, obtained from direct and indirect methods are more related to the direction of tensile stress with respect to the layer interfaces. The directions of tensile stress in the direct tension test and the splitting test are generally perpendicular and parallel to those of the layer interfaces, respectively. In the configuration used during desiccation test, the cracks occur perpendicularly to the interface (as experienced during indirect tensile test). Finally, indirect tensile test has the main advantage of being a conventional geomechanical test, that makes our methodology straightforward. At the end, the methodology requires three conventional characterizations: the uniaxial compression test, indirect tensile test and water retention curve.

6. Conclusions

Desiccation cracking occurs when the tensile stress overpasses the tensile strength of the material. Both parameters depend on suction. The tensile stress is induced by the constrained deformation upon drying. Consequently, it is a function of the soil stiffness that evolves during drying. The problem is highly coupled and the concept of unsaturated soil mechanics must be used to analyse the observed results. In the present study, effective stress framework for unsaturated soils is used with the χ parameter expressed as a power law of the degree of saturation. The α coefficient (exponent of the degree of saturation to express the χ parameter) is calibrated to fulfil the uniqueness of the shear failure criterion expressed in this effective stress formalism, whatever the suction level.

In order to provide the required material parameters for the analysis, indirect tensile tests, uniaxial compression tests, free shrinkages and constrained shrinkages have been carried out on
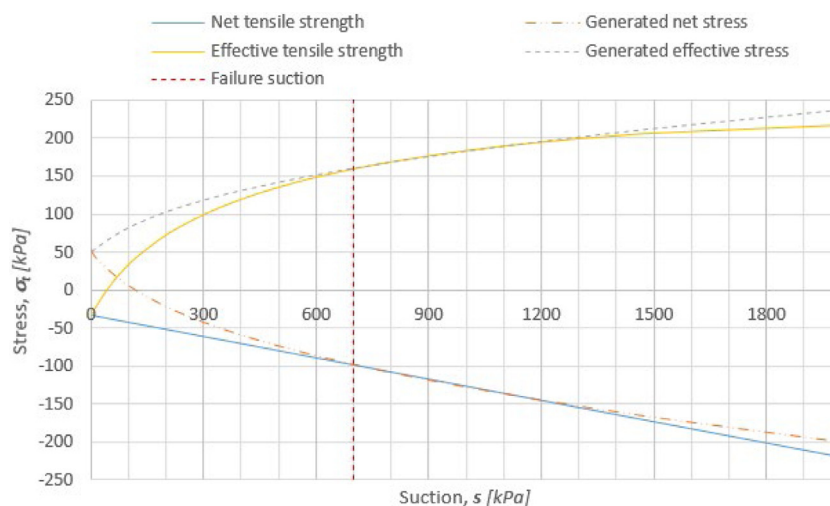
Fig. 23. Evolution of tensile stress and strength as a function of suction during constrained shrinkage of untreated specimen (compression is positive).
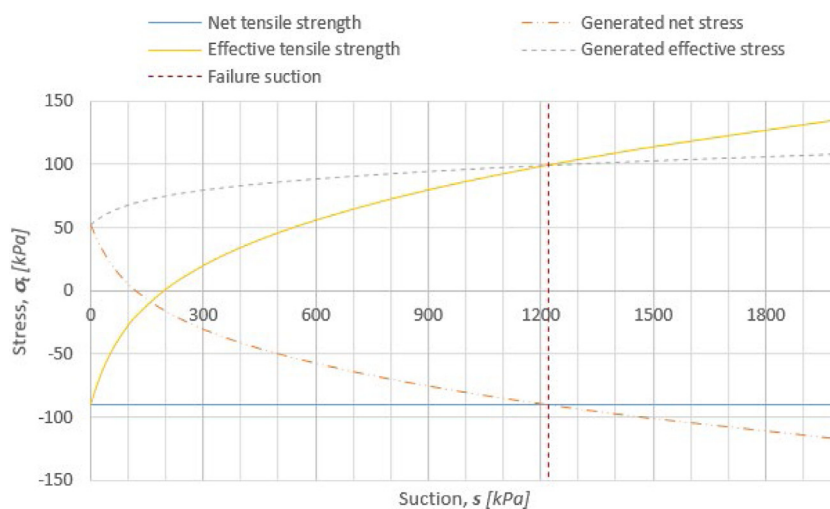

Fig. 24. Evolution of tensile stress and strength as a function of suction during constrained shrinkage of treated specimen (compression is positive).

compacted untreated and lime-treated silty clay soil. It is demonstrated that the constitutive framework, using an effective stress formalism for unsaturated soils, is able to reproduce the experienced volumetric strain upon free shrinkage and crack occurrence upon constrained shrinkage. All the required parameters of this constitutive framework are deduced from independent tests and the blind prediction of strain upon free shrinkage and crack occurrence upon constrained shrinkage are in good agreement with experimental observations.

For the tested soil, lime treatment (with 2% of lime) postpones (in terms of suction levels) the triggering of desiccation cracks. For a drying at 1000 kPa of suction, untreated soil exhibits the development of a clear tensile crack while treated soil remains un-cracked until 1500 kPa of suction upon the same constrained conditions. This is well reproduced by the constitutive model.

CRediT authorship contribution statement

Nicolas Poncelet: Validation, Formal analysis, Investigation, Data curation, Writing – original draft, Writing - review & editing, Visualization. **Gontran Herrier:** Resources, Formal analysis, Investigation, Writing – original draft. **Bertrand François:** Conceptualization, Methodology, Supervision, Project administration, Funding acquisition, Writing – original draft, Writing - review & editing.

Declaration of competing interest

The authors declare that they have no known competing financial interests or personal relationships that could have appeared to influence the work reported in this paper.

References

1. Little DN. *Stabilization of Pavement Subgrades and Base Courses with Lime.* Dubuque, IA, US: Kendall/Hunt publication Company; 1995.
2. Peron H. *Desiccation Cracking of Soils* (Doctoral dissertation). Lausanne, Switzerland: Ecole Polytechnique Fédérale de Lausanne; 2008.
3. Peron H, Laloui L, Hu LB, Hueckel T. Formation of drying crack patterns in soils: a deterministic approach. *Acta Geotech.* 2013;8(2):215–221.
4. Konrad JM, Ayad R. Desiccation of a sensitive clay: field experimental observations. *Can Geotech J.* 1997;34(6):929–942.
5. Kodikara J, Costa S. Desiccation cracking in clayey soils: mechanisms and modelling. In: *Multiphysical Testing of Soils and Shales.* Berlin, Heidelberg: Springer; 2013:21–32.
6. Colina H, Roux S. Experimental model of cracking induced by drying shrinkage. *Eur Phys J E.* 2000;1(2–3):189–194.
7. Corte A, Higashi A. *Experimental Research on Desiccation Cracks in Soil, (No. RR-66).* Hanover NH: Cold regions research and engineering Lab; 1964.
8. Hueckel TA. Water–mineral interaction in hygromechanics of clays exposed to environmental loads: a mixture-theory approach. *Can Geotech J.* 1992;29(6):1071–1086.
9. Murray RS, Quirk JP. Intrinsic failure and cracking of clay. *Soil Sci Am J.* 1990;54(4):1179–1184.

10. Scherer GW. Theory of drying. *J Am Ceram Soc.* 1990;73(1):3–14.
11. Corte A, Higashi A. *Experimental Research on Desiccation Cracks in Soil-Research.* Report 66, Wilmette, Illinois: US Army Snow Ice and Permafrost Research Establishment; 1960.
12. Delage P, Howat MD, Cui YJ. The relationship between suction and swelling properties in a heavily compacted unsaturated clay. *Eng Geol.* 1998;50(1–2):31–48.
13. Groisman A, Kaplan E. An experimental study of cracking induced by desiccation. *Europhys Lett.* 1994;25(6):415.
14. Lachenbruch AH. Depth and spacing of tension cracks. *J Geophys Res.* 1961;66(12):4273–4292.21.
15. Lau JTK. *Desiccation Cracking of Soils* (Doctoral dissertation). Saskatoon, Canada: University of Saskatchewan; 1987.
16. Lloret A, Ledesma A, Rodriguez R, Sanchez MJ, Olivella S, Suriol J. *Crack Initiation in Drying Soils.* In: Unsaturated Soils, Pékin; 1998.
17. Miller CJ, Mi H, Yesiller N. Experimental analysis of desiccation crack propagation in clay liners 1. *JAWRA J Am Water Resour Assoc.* 1998;34(3):677–686.
18. Tang CS, Cui YJ, Tang AM, Shi B. Experiment evidence on the temperature dependence of desiccation cracking behavior of clayey soils. *Eng Geol.* 2010;114(3–4):261–266.
19. Tang CS, Shi B, Liu C, Gao L, Inyang HI. Experimental investigation of the desiccation cracking behavior of soil layers during drying. *J Mater Civ Eng.* 2011;23(6):873–878.
20. Mitchell JK, Soga K. *Fundamentals of Soil Behavior, Vol. 3.* New York: John Wiley & Sons; 2005.
21. Costa S, Kodikara JK, Shannon B. Salient factors controlling desiccation cracking of clay in laboratory experiments. *Géotechnique.* 2013;63(1):18–29.
22. Kodikara JK, Barbour SL, Fredlund DG. Desiccation cracking of soil layers. *Unsaturated Soils Asia.* 2000;90(5809):139.
23. Wei X, Hattab M, Bompard P, Fleureau JM. Highlighting some mechanisms of crack formation and propagation in clays on drying path. *Géotechnique.* 2016;66(4):287–300.
24. Yesiller N, Miller CJ, Inci G, Yaldo K. Desiccation and cracking behavior of three compacted landfill liner soils. *Eng Geol.* 2000;57(1–2):105–121.
25. Sanchez M, Atique A, Kim S, Romero E, Zielinski M. Exploring desiccation cracks in soils using a 2D profile laser device. *Acta Geotech.* 2013;8(6):583–596.
26. Alonso EE, Pinyol NM, Gens A. Compacted soil behaviour: initial state, structure and constitutive modelling. *Géotechnique.* 2013;63(6):463–478.
27. Gerard P, Mahdad M, McCormack AR, François B. A unified failure criterion for unstabilized rammed earth materials upon varying relative humidity conditions. *Constr Build Mater.* 2015;95:437–447.
28. Van Genuchten MT, Nielsen D. On describing and predicting the hydraulic properties. *Ann Geophys.* 1985;3(5):615–628.
29. Bishop AW, Henkel DJ. *The Measurement of Soil Properties in the Triaxial Test.* London: William Clowes and Sons; 1969:228.
30. Lade PV. *Triaxial Testing of Soils.* John Wiley & Sons; 2016.
31. Kouassi P, Breysse D, Girard H, Poulain D. A new technique of kneading compaction in the laboratory. *Geotech Test J.* 2000;23(1):72–82.
32. ASTM. *D 3967-08: Standard Test Method for Splitting Tensile Strength of Intact Rock Core Specimens.* West Conshohocken, USA: ASTM International; 2008.
33. Peron H. *Desiccation Cracking of Soils* (PhD dissertation). Lausanne: EPFL; 2008.
34. Shin H, Santamarina JC. Desiccation cracks in saturated fine-grained soils: particle-level phenomena and effective-stress analysis. *Geotechnique.* 2011;61:961–972.
35. Hueckel T, Mielniczuk B, El Youssoufi MS, Hu LB, Laloui L. A three-scale cracking criterion for drying soils. *Acta Geophys.* 2014;62(5):1049–1059.
36. Araki H, Koseki J, Sato T. Tensile strength of compacted rammed earth materials. *Soils Found.* 2016;56(2):189–204.